HEFAT2012
9th International Conference on Heat Transfer, Fluid Mechanics and Thermodynamics
16 – 18 July 2012
Malta

MODELING COMBINED CYCLE PERFORMANCE AT FULL AND PART LOADS

N.A. Ali and A.Y. Abdalla*
*Author for correspondence
Mechanical Engineering Department, College of Engineering,
University of Bahrain,
P.O. Box 32038,
Bahrain,
E-mail: ayabdalla@eng.uob.bh

ABSTRACT

A block of 460 MW (two gas turbines and one steam turbine) combined cycle power plant has been modeled and simulated. The model equations have been solved by the constructed MATLAB computer program. The model accounts for the actual operating parameters within the block components; compressor, combustion chamber, gas turbine, HRSG and steam turbine. The developed program is utilized to investigate the effect of load, and heat losses in the combustion chamber on the block performance. To validate the present model, the gas turbine performances at different loads are calculated. The results of the present model are compared with the corresponding ones given by the block's manufacturer. The comparison has shown that the deviations are in the range of 3-5%. Exergy analysis is performed based on the first and second laws of thermodynamics. Its results have shown that the maximum exergy destruction is found to be in the combustion chamber at full and part loads.

The effects of the percentage of heat losses within the combustion chamber on the fuel consumption, gas turbine cycle efficiency and turbine work net are investigated. The fuel mass flow rate and work net of the gas turbine increase as the heat losses increase while the thermal efficiency decreases.

INTRODUCTION

The needs of continuous save supply of the fossil fuel and the issue of global warming play a vital role in the development and use of the combined power plant. As it has a better performance than a gas or steam turbine power plants furthermore studies have been performed in this field nowadays in order to improve the efficiency more. One method of measuring the performance of a power plant is based on the conservation of mass and energy principle, which is the first law of thermodynamic. This method, unfortunately, does not cover complete evaluation because it is not indicating how much the energy is utilized within the plant [1]. The second method is the exergy analysis which bases on the second law of thermodynamic. It measures the quality of

NOMENCLATURE

c_p	[kJ/kgK]	Specific heat
$\dot{E}x$	[MW]	Exergy flow rate
$\dot{E}x_d$	[MW]	Exergy destruction rate
h	[kJ/kg]	Specific enthalpy
HL	[%]	Heat losses within combustion chamber
LHV	[kJ/kg]	Lower heating value
$\dot{m}$	[kg/s]	Mass flow rate
MW	[kg/kmol]	Molecular weight
N	[kmol]	Number of moles
P	[bar]	Pressure
$\dot{Q}$	[MW]	Heat energy transfer
R	[kJ/kgK]	Gas constant
r_c	[-]	Pressure ratio
s	[kJ/kgK]	Specific entropy
T	[K]	Temperature
$\dot{W}$	[MW]	Power
y_d	[-]	Exergy destruction ratio
y^*_d	[-]	Exergy destruction rate

Special characters

γ	[-]	Specific heat ratio
ε	[-]	Exergetic efficiency
η	[%]	Efficiency
λ	[%]	Percent of excess air
φ	[-]	Fuel air equivalence ratio

Subscripts

c	Compressor
cc	Combustion chamber
dea	Deaerator
exh	Exhaust steam from steam turbine
ext	Extraction steam from steam turbine
HP	High pressure
LP	Low pressure
o	Ambient condition
p	Polytropic
t	Turbine
s	Steam

energy as well as its quantity [2], so it can guides how to utilized within the plant. The worldwide efforts are being develop the gas turbine and combined cycle technology in order to meet the higher operational efficiency of power generation plants.

The exergy analysis of a combined power plant has been presented by previously by Ahmadi and Dincer [3] and Sanjay [4]. The calculation of the exergy can show the main location of exergy losses, their origins and also, identifies the components or processes, where the highest destruction of exergy appears. This helps in finding away to reduce it and hence the performance will improve. Reddy and Mohamed [5] analyzed a natural gas fired combined cycle power plant to investigate the effect of gas turbine inlet temperature and pressure ratio on the exergetic efficiency.

The present study is aimed to investigate the performance of a combined cycle power plant operates at part loads. In the combined cycle plant the gas turbine is the top cycle and the steam turbine is the bottom cycle. The steam turbine output depends on the gas turbine load. There are two ways of changing the gas turbine geometry for controlling the load either by compressor variable inlet guides vans (VIGVs) and turbine variable area nozzle (VAN) [6].

The use of VIGVs to control the part load has been presented previously [7] and [8]. The advantage of VIGVs is to control the exhaust gas temperature of gas turbine so it does not exceed the allowable value. This is achieved by controlling the compressor inlet air flow during the part loads operation. Consequently, it does enhance the heat recovery for the bottom cycle [8].

In this present paper, the effect of the load on the ratio of mass flow rate of the steam to the mass of the exhaust gases where investigated. The effect of heat losses within the combustion chamber and pressure ratio on the gas turbine and block performance are reported. Furthermore, the exergy losses at full and part loads in the compressor, combustion chamber, gas turbine, heat recovery steam generation, deaerator, feed water pumps, steam turbine, air cooled condenser, condensate pumps, ejector and feed water heater are analyzed, so it is possible to identify where the largest quantity of exergy destruction occurs within the plant.

SYSTEM

The system presented in this work is 460 MW combined cycle power plant (two gas turbines and one steam turbine) and details of the system components are shown in Figure 1. The plant is consisted of two identical ALSTOM 13E2 gas turbines (GT) and one KA13E2-2 ALSTOM steam turbine (ST). The exhaust gas from each gas turbine is diverted to heat recovery steam generator (HRSG). The generated steam from the two HRSG's enters steam turbine (ST). The steam cycle utilizes regenerative feed water heating system. Feed water heating is mainly carried out in Low pressure pre-heater heat exchanger (LP Pre-heater) along with deareator serves as an open feed water heater. The feed water is supplied to HRSGs at two levels of pressure which are high pressure (HP) and low pressure (LP). High pressure feed water pumps (HPFWPs) and low pressure feed water pumps (LPFWPs), respectively are used to feed water. The HP and LP steam are generated by HRSGs and used to drive the steam turbine. The turbine exhaust is sent to the air cooled condenser (ACC) and the condensate to the condensate recovery tank (CRT). Finally, the condensate is circulated through the condensate extraction pumps (CEPs). Then, the cycle starts over again.

MODEL

A model is developed to simulate, the combined cycle power plant, a block (system) it consists of two gas turbines and one steam turbine. A MATLAB program is constructed and used to solve the equations that represent each component of the system. The details of the model equations are below:

In the present work, the specific heat of gas at constant pressure is defined as a function of temperature, given by the polynomial taken from [9].

$$c_p(T) = R_u\,(a_1 + a_2T + a_3T^2 + a_4T^3 + a_5T^4) \qquad (1)$$

The coefficients (a_1, a_2, ...) of the different species are given in Table 1. Then, the enthalpy and the entropy of gas turbine working fluid are calculated using the above function in the following equations:

$$h(T) = \int c_p(T)\,dT \qquad (2)$$

$$s(T,P) = \int c_p(T).\frac{dT}{T} - R_u\,ln\frac{P}{P_a} \qquad (3)$$

Where R_u is universal gas constant which is equal to 8.314 kJ/kmol.K.

Table 1 The coefficients of Eq. 1 of the different species

Species	a_1	$a_2.10^2$	$a_3.10^6$	$a_4.10^9$	$a_5.10^{14}$
Temperature range from 250 to 1000K					
N_2	3.299	0.141	-3.963	5.642	-244.485
O_2	3.213	0.113	-0.576	1.314	-87.686
CO_2	2.276	0.992	-10.409	6.867	-211.728
Ar	2.500	0	0	0	0
H_2O	3.387	0.347	-6.355	6.969	-250.659
Temperature range above 1000K					
N_2	2.927	0.149	-0.568	0.101	-0.675
O_2	3.698	0.061	-0.126	0.018	-0.114
CO_2	4.454	0.314	-1.278	0.239	-1.669
Ar	2.500	0	0	0	0
H_2O	2.672	0.306	-0.873	0.120	-0.639

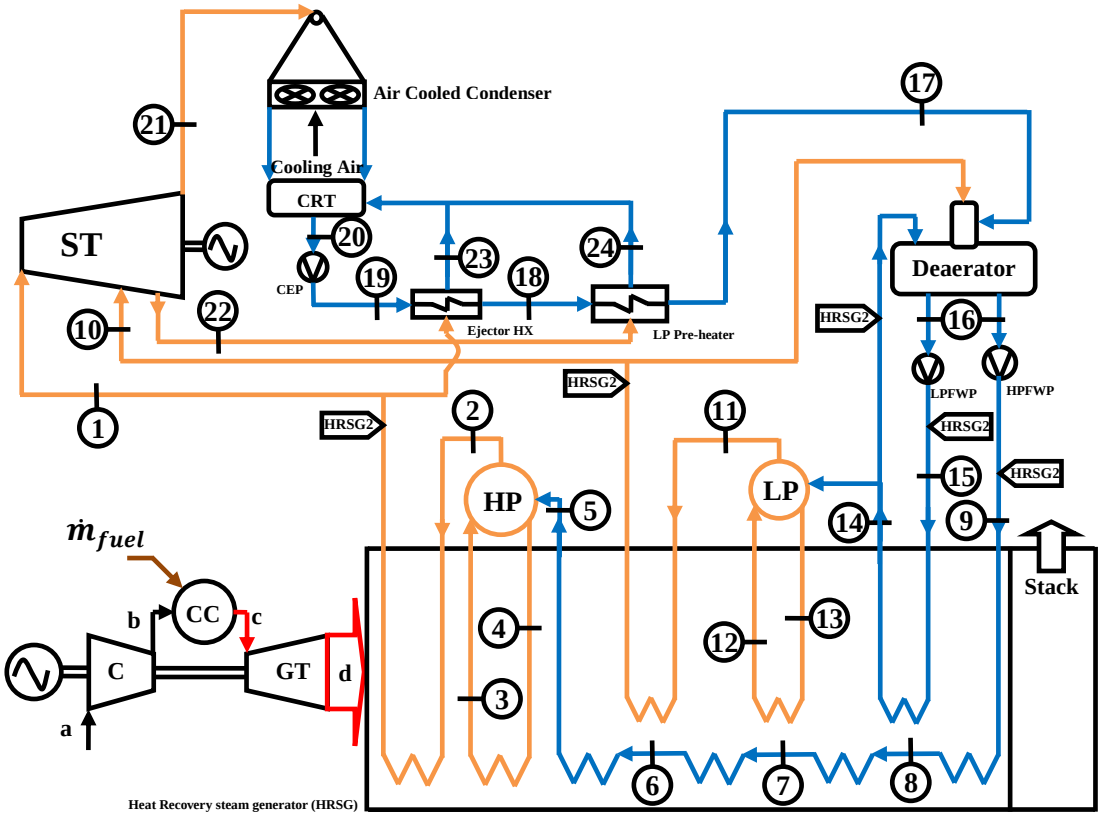

Figure 1 Schematic diagram of the combined power plant

ENERGY ANALYSIS:

The energy balance equations for various parts of the combined cycle power plant are described as follows:

1. Air compressor model:

The atmospheric air is drawn and compressed in axial-flow multi stage compressor. The compression process is assumed to be polytropic process taking polytropic efficiency ($\eta_{p,c}$) as 90%. The compressor discharge temperature (T_b) is calculated as a function of inlet temperature (T_a), compressor pressure ratio (r_c) and polytropic efficiency, by the Eq. (4) taken from [10]:

$$T_b = T_a . (r_c)^{(\gamma-1)/\gamma\eta_{p,c}} \quad (4)$$

Where η_c is the isentropic efficiency and is calculated from [10]:

$$\eta_c = \frac{1-r_c^{(\gamma-1)/\gamma}}{1-r_c^{(\gamma-1)/\gamma\eta_{p,c}}} \quad (5)$$

The energy balance of the air compressor is described as follow:

$$-\dot{W}_c = \dot{m}_{air}(h(T_b) - h(T_a)) \quad (6)$$

2. Combustion chamber model:

The mass and energy balance of the combustion chamber for the given turbine inlet temperature (TIT) is expressed by the following equations correspondingly:

$$\dot{m}_{air} + \dot{m}_{fuel} = \dot{m}_{gas} \quad (7)$$

$$\dot{m}_{fuel}\, LHV\, \eta_{cc}\, (1 - HL) + \dot{m}_{air}\, h_b = \dot{m}_{gas}\, h_c \quad (8)$$

The mass flow rate of fuel ($\dot{m}_{fuel}$) which is required to achieve the desire TIT is obtained from combustion reaction equations, for the used gas fuel which is Khuff gas (Local fuel). Its compositions are given in Table 2. The analysis of the fuel is supplied from Bapco (The local company supplies the fuel to all the power plants in Bahrain). The reaction equations are:

$$R_{CH_4}CH_4 + R_{C_2H_6}C_2H_6 + R_{C_3H_8}C_3H_8 + R_{C_4H_{10}}C_4H_{10} + R_{C_5H_{12}}C_5H_{12} + R_{C_6H_{14}}C_6H_{14} + R_{N_2}N_2 + R_{CO_2}CO_2 + a_{actual}(O_2 + \frac{n_{N_2}}{n_{O_2}}N_2 + \frac{n_{H_2O}}{n_{O_2}}H_2O + \frac{n_{CO_2}}{n_{O_2}}CO_2 + \frac{n_{Ar}}{n_{O_2}}Ar) \rightarrow (y_{O_2}O_2 + y_{N_2}N_2 + y_{H_2O}H_2O + y_{CO_2}CO_2 + y_{Ar}Ar) \quad (9)$$

Where $N_{air} = (1 + \frac{n_{N_2}}{n_{O_2}} + \frac{n_{H_2O}}{n_{O_2}} + \frac{n_{CO_2}}{n_{O_2}} + \frac{n_{Ar}}{n_{O_2}})$ is the number of air moles.

The equivalence fuel air ratio φ is defined as:

$$\varphi = \frac{1}{1+\lambda} \quad (10)$$

Where λ is percent excess air.

The fuel air ratio is calculated as follow:

$$(FA)_{actual} = \varphi . (FA)_{stoic} \quad (11)$$

$$a_{actual} = \frac{MW_{fuel}}{MW_{air}} . \frac{1}{N_{air}} . \frac{1}{(FA)_{actual}} \quad (12)$$

The different species molar fractions are calculated as following:

$$y_{CO_2} = R_{CH_4} + 2R_{C_2H_6} + 3R_{C_3H_8} + 4R_{C_4H_{10}} + 5R_{C_5H_{12}} + 6R_{C_6H_{14}} + R_{CO_2} + a_{actual}.\frac{n_{CO_2}}{n_{O_2}} \quad (13)$$

$$y_{H_2O} = 2R_{CH_4} + 3R_{C_2H_6} + 4R_{C_3H_8} + 5R_{C_4H_{10}} + 6R_{C_5H_{12}} + 7R_{C_6H_{14}} + a_{actual}.\frac{n_{H_2O}}{n_{O_2}} \quad (14)$$

$$y_{N_2} = R_{N_2} + a_{actual}.\frac{n_{N_2}}{n_{O_2}} \quad (15)$$

$$y_{Ar} = a_{actual}.\frac{n_{Ar}}{n_{O_2}} \quad (16)$$

Table 2 The used fuel composition and its lower heating values

Compositions	LHV (kJ/kg)	Mole %
Methane, CH_4	50,016	79.49
Ethane, C_2H_6	47,489	1.52
Propane, C_3H_8	46,357	0.36
N-Butane, C_4H_{10}	45,742	0.17
N-Pentane, C_5H_{12}	45,355	0.09
Hexane Plus, C_6H_{14}	45,105	0.25
Nitrogen, N_2	-	11.74
Carbon Dioxide, CO_2	-	6.38
Total	34471*	100

*The lower heating value of the fuel is lower than what is reported in the literature for the natural gas because the Khuff gas has lower energy content than a normal natural gas.

$$y_{O_2} = 2R_{CO_2} + a_{actual}.(2 + 2\frac{n_{CO_2}}{n_{O_2}} + \frac{n_{H_2O}}{n_{O_2}}) - 2y_{CO_2} - y_{H_2O} \quad (17)$$

The a_{stoich} is the stoichiometric quantity of oxidizer, and it is calculated from:

$$a_{stoich} = 2R_{CH_4} + 3.5R_{C_2H_6} + 5R_{C_3H_8} + 6.5R_{C_4H_{10}} + 8R_{C_5H_{12}} + 9.5R_{C_6H_{14}} \quad (18)$$

$$(FA)_{stoich} = \frac{MW_{fuel}}{MW_{air}}.\frac{1}{N_{air}}.\frac{1}{a_{stoich}} \quad (19)$$

3. Gas turbine model:

The hot gases leave the combustion chamber are expanded in turbine. The expansion process is assumed to be polytropic process taking polytropic efficiency as 95%. The turbine exhaust temperature (TET) has been calculated from inlet turbine temperature (TIT), expansion pressure ratio ($\frac{P_d}{P_c}$) and turbine polytropic efficiency ($\eta_{p,t}$), by Eq. (20):

$$TET = TIT.(\frac{P_d}{P_c})^{(\gamma-1).\eta_{p,t}/\gamma} \quad (20)$$

Where is (η_t) the turbine isentropic efficiency and calculated from [10]:

$$\eta_t = \frac{1-(\frac{P_d}{P_c})^{(\gamma-1).\eta_{p,t}/\gamma}}{1-(\frac{P_d}{P_c})^{(\gamma-1)/\gamma}} \quad (21)$$

The energy balance of the gas turbine is described as follow:

$$\dot{W}_t = \dot{m}_{gas}(h(TIT) - h(TET)) \quad (22)$$

The work net from the gas turbine is equal to:

$$\dot{W}_{net} = \dot{W}_t - \dot{W}_c \quad (23)$$

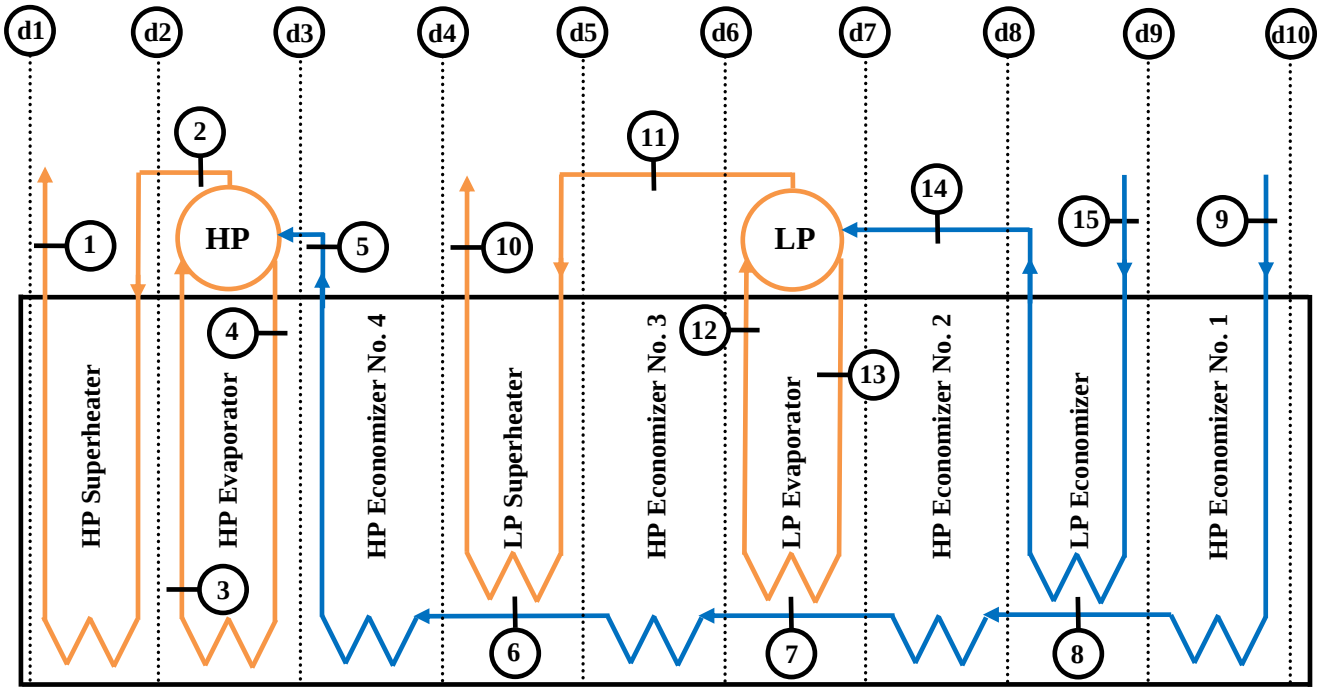

Figure 2 Details of heat recovery steam generation

4. Heat recovery steam generator (HRSG) model:

A dual pressure HRSG shown in Figure 2 is analyzed by applying the mass and energy balance equation for water and gas at each part of HRSG.

High-pressure superheater:

$$\dot{m}_{s,HP}(h_1 - h_2) = \dot{m}_{gas}(h_{d1} - h_{d2}) \quad (24)$$

High-pressure evaporator:

$$\dot{m}_{s,HP}(h_3 - h_4) = \dot{m}_{gas}(h_{d2} - h_{d3}) \quad (25)$$

High-pressure economizer No. 4:

$$\dot{m}_{s,HP}(h_5 - h_6) = \dot{m}_{gas}(h_{d3} - h_{d4}) \quad (26)$$

Low-pressure superheater:

$$\dot{m}_{s,LP}(h_{10} - h_{11}) = \dot{m}_{gas}(h_{d4} - h_{d5}) \quad (27)$$

High-pressure economizer No. 3:

$$\dot{m}_{s,HP}(h_6 - h_7) = \dot{m}_{gas}(h_{d5} - h_{d6}) \quad (28)$$

Low-pressure evaporator:

$$\dot{m}_{s,LP}(h_{12} - h_{13}) = \dot{m}_{gas}(h_{d6} - h_{d7}) \quad (29)$$

High-pressure economizer No. 2:

$$\dot{m}_{s,HP}(h_7 - h_8) = \dot{m}_{gas}(h_{d7} - h_{d8}) \quad (30)$$

Low-pressure economizer:

$$(\dot{m}_{s,LP} + \dot{m}_{dea,LP})(h_{14} - h_{15}) = \dot{m}_{gas}(h_{d8} - h_{d9}) \quad (31)$$

High-pressure economizer No. 1:

$$\dot{m}_{s,HP}(h_8 - h_9) = \dot{m}_{gas}(h_{d9} - h_{d10}) \quad (32)$$

5. Steam turbine model:

The steam turbine work is calculated from the energy balance equation as described in the following:

$$(2\dot{m}_{s,HP} - \dot{m}_{ejector}).h_1 + (2\dot{m}_{s,LP} - \dot{m}_{dea,st}).h_{10} - \dot{m}_{ext}.h_{22} - \dot{m}_{exh,ST}.h_{21} = \dot{W}_{ST} \quad (33)$$

6. Deaerator model:

The energy balance of the deaerator is described as follow:

$$2\dot{m}_{dea,LP}.h_{14} + \dot{m}_{dea,st}.h_{10} + (2.(\dot{m}_{s,HP} + \dot{m}_{s,LP}) + \dot{m}_{dea,LP}).h_{17} = 2.(\dot{m}_{s,HP} + \dot{m}_{s,LP} + \dot{m}_{dea,LP}).h_{16} \quad (34)$$

Where $h_{17} = h_f(T_{dea})$

7. LP pre-heater model:

The energy balance of the LP pre-heater is described as follow:

$$(2.(\dot{m}_{s,HP} + \dot{m}_{s,LP}) + \dot{m}_{dea,LP}).(h_{17} - h_{18}) = \dot{m}_{ext}.(h_{22} - h_{24}) \quad (35)$$

8. Ejector heat exchanger model:

The energy balance of the ejector heat exchanger is described as follow:

$$(2.(\dot{m}_{s,HP} + \dot{m}_{s,LP}) + \dot{m}_{dea,LP}).(h_{18} - h_{19}) = \dot{m}_{ejector}.(h_1 - h_{23}) \quad (36)$$

9. Air cooled condenser (ACC) model:

In the present work, the condenser is an air cooled condenser. It is basically a cross flow heat exchanger consists of four "A" roof type streets of finned tubes elements. The axial flow fans, locate underneath the roof, force the air through the fins. The numbers of operating fans are depended on the steam back pressure and ambient temperature.

The steam temperature is assumed to be equal the tube surface temperature i.e. the effect of tube thickness is negligible. Therefore, the condensate steam temperature can be found as follow [11]:

$$T_{ACC,steam} = T_{air,in} + \Delta T_{LM}\left(\frac{A_{ACC}.\bar{\alpha}_{air}}{\dot{m}_{air,ACC}.c_{p,air}}\right) / \left\{1 - exp\left(\frac{-A_{ACC}.\bar{\alpha}_{air}}{\dot{m}_{air,ACC}.c_{p,air}}\right)\right\} \quad (37)$$

The pressure of air cooled condenser is the saturated pressure at $T_{ACC,steam}$.

Where, the heat transfer coefficient at air side ($\bar{\alpha}_{air}$) can be calculated as follow [11]:

$$\bar{\alpha}_{air} = \frac{\overline{N_u}.k_{air}}{D_r} \quad (38)$$

Where D_r is the external diameter of the tube at fin root.

The recommended correlation Nusselt number ($\overline{N_u}$) for in-line, high-fin tube arrays taken from [11] and is given by:

$$\overline{N_u} = 0.269\, Re^{0.625}\left(\frac{A_f}{A_T}\right)^{-0.375} P_r^{0.333} \quad (39)$$

Where P_r is the air Prandtl number as a function of air temperature T and is given by [9]:

$$P_r(T) = 1.2 \times 10^{-6}.T^2 - 9.2 \times 10^{-4}.T + 0.875 \quad (40)$$

The surface area of the finned tubes (n_t) of length (L_t) is given by:

$$A_f = \frac{\pi\, n_t\, L_t}{(s_f + w_f)}\left\{\frac{1}{2}\left(D_f{}^2 - D_r{}^2\right) + D_f\, w_f + D_r s_f\right\} \quad (41)$$

Where s_f, w_f, and D_f are fins pitch, fins thickness, and outer diameter of fins, respectively.

The total tube surface area without fins is:

$$A_T = \pi\, n_t\, L_t D_r \quad (42)$$

The Air thermal conductivity (k_{air}) is a function of air temperature T and is given by [9]:

$$k_{air}(T) = 3.13908 \times 10^{-9}.T^3 - 3.40606 \times 10^{-5}.T^2 + 9.78225 \times 10^{-2}.T - 0.10903 \quad (43)$$

The Reynolds number (Re) is calculated as follow:

$$Re = \frac{V_{max} D_r\, \rho_{air}}{\mu_{air}} \quad (44)$$

Where μ_{air} is air dynamic viscosity at air temperature $T$and it is given by [9]:

$$\mu_{air}(T) = \mu_o \frac{(T_o + C_o)}{(T + C_o)}.\left(\frac{T_o}{T}\right)^{1.5} \quad (45)$$

Where T_o, C_o and μ_o are constant and equal to 291.15K, 120K and $18.27 \times 10^{-6}\ Pa.s$, respectively.

The maximum flow velocity (V_{max}) taken from [11] and is given by:

$$V_{max} = \frac{\dot{m}_{air,ACC}}{\rho_{air}\, S_{min}} \quad (46)$$

The minimum flow area (S_{min}) for most cross-flow heat exchanger, is perpendicular to the flow direction taken from [11] and is given by:

$$S_{min} = n_t L_t (p_t - D_r - \frac{2 w_f h_f}{(w_f + s_f)}) \quad (47)$$

Where p_t is tubes pitch in plane perpendicular to flow.

The total axial flow fans mass flow rate is calculated as follows:

$$\dot{m}_{air,ACC} = n_{fan}.v_{fan}.\rho_{air} \quad (48)$$

Where n_{fan}, v_{fan}, and ρ_{air} are number of fans, fan volume flow rate, and air density, respectively.

The energy balance of the ACC is described as follow:

$$\dot{m}_{air,ACC}\left(T_{air,ACC_{out}} - T_{air,ACC_{in}}\right) = \dot{m}_{exh,ST}.(h_{21} - h_{20}) \quad (49)$$

EXERGY ANALYSIS:

Exergy is defined as the maximum theoretical useful work obtained as the system interacts with the environment state without violating any thermodynamic laws [12].

In the present work, the dead state condition (15℃, 1.013 bar and 60% relative humidity with its dry air composition chemical mole fraction N_2, O_2, CO_2 and Ar as 78.084%, 20.947%, 0.035% and 0.934% respectively) is chosen for as thermo-mechanical and chemical equilibrium condition for the exergy analysis.

For a control volume the specific exergy has been calculated by the following equation [13] is given by

$$\dot{E}x_Q + \sum_i \dot{m}_i.ex_i = \sum_e \dot{m}_e.ex_e + \dot{E}x_W + \dot{E}x_d \quad (50)$$

Where the subscripts i and e are the specific exergy of control volume inlet and exit, and $\dot{E}x_d$ is the exergy destruction. Where $\dot{E}x_Q$ and $\dot{E}x_W$ are exergy of heat transfer and work respectively which cross the boundaries.

$$\dot{E}x_Q = \sum_j (1 - \frac{T_o}{T_j}).\dot{Q}_j \quad (51)$$

$$\dot{E}x_W = \dot{W} \quad (52)$$

The total exergy rate ($\dot{E}x$) is divided into four main components which define as follow:

$$\dot{E}x = \dot{E}x_{ph} + \dot{E}x_{ch} + \dot{E}x_{potential} + \dot{E}x_{kinetic} \quad (53)$$

$$\dot{E}x = \dot{m}.ex \quad (54)$$

In the present work, the potential ($\dot{E}x_{potential}$) and kinetic ($\dot{E}x_{kinetic}$) exergy are assumed to be negligible as the evaluation and speed changes influences are negligible. The other two components $\dot{E}x_{ph}$ and $\dot{E}x_{ch}$ are physical and chemical exergy respectively.

$$Ex_{ph} = \dot{m}.[(h - h_o) - T_o(s - s_o)] \quad (55)$$

The mixture of chemical exergy is defined as follows:

$$Ex^{ch}_{mix} = \dot{m}.(\sum_{i=1}^{n} x_i.ex_i^{ch} + RT_o \sum_{i=1}^{n} x_i.\ln x_i) \quad (56)$$

Where x_i is mole fraction of a species.

Fuel exergy:

The fuel exergy is a combination of physical ($\dot{E}x_{ph}$) and chemical ($\dot{E}x^{ch}_{mix}$) exergy, and they are taken from [11].

$$\dot{E}x_{ph} = \dot{m}_{fuel}\left[c_p^{-h}(T - T_o) - T_o\left\{c_p^{-s}\ln(\frac{T}{T_o}) - R\ln(\frac{P}{P_o})\right\}\right] \quad (57)$$

Where,

$$c_p^{-h} = \frac{1}{T - T_o}\int_{T_o}^{T} c_p dT \text{ and } c_p^{-s} = \frac{1}{\ln(\frac{T}{T_o})}\int_{T_o}^{T} c_p \frac{dT}{T}$$

c_p^{-h} and $c_p^{-s}$are mean molar isobaric exergy capacity for evaluating enthalpy and entropy changes.

$$\dot{E}x^{ch}_{mix} = \dot{m}_{fuel}[\sum_{i=1}^{n} x_i.ex_i^{ch} + RT_o \sum_{i=1}^{n} x_i.\ln x_i] \quad (58)$$

$$\dot{E}x_{fuel} = \dot{E}x_{ph} + \dot{E}x^{ch}_{mix} \quad (59)$$

The exergy destruction of the kth component in the system can be written as the difference between fuel ($\dot{E}x_{f,k}$) and product ($\dot{E}x_{p,k}$) exergy of the kth component in the system [15]:

$$\dot{E}x_{d,k} = \dot{E}x_{f,k} - \dot{E}x_{p,k} \quad (60)$$

In addition to exergy destruction $\dot{E}x_d$, the exergetic efficiency and two exergy destruction ratios are presented in this work [15] and [16]

The exergetic efficiency (ε_k) of the kth component is the ratio of the product exergy ($\dot{E}x_{p,k}$) to the fuel exergy ($\dot{E}x_{f,k}$):

$$\varepsilon_k = \frac{\dot{E}x_{p,k}}{\dot{E}x_{f,k}} \quad (61)$$

The exergy destruction ratio $y_{d,k}$ is the ratio compares the exergy destruction in the kth component with total fuel exergy supplied $\dot{E}x_{fuel}$ to overall the system:

$$y_{d,k} = \frac{\dot{E}x_{d,k}}{\dot{E}x_{fuel}} \quad (62)$$

On the other hand, the exergy destruction rate of the kth component can be compared to the total exergy destruction ($\dot{E}x_{d,Total}$) (Sum of all k components in the system):

$$y^*_{d,k} = \frac{\dot{E}x_{d,k}}{\dot{E}x_{d,Total}} \quad (63)$$

MODEL VALIDATION

The MATLAB program is run to produce the results of the given system, shown Figure 1. The input data at the design point used in the present work to run the thermodynamic simulation program are given Table 3. The data cover, the compressor, combustion chamber, the gas turbine, heat recovery steam generator and its components, steam turbine, and air cooled condenser. The program is used to re-produce the power at the full and the part load for the gas turbine (Top cycle) because the performance of the combined cycle depends mainly on the performance of the gas turbine. The obtained results from the present model for the gas turbine power are given in Table 4 along with those given by the manufacture. The deviations between the calculated power of the gas turbine and the actual ones are in the range of 3-5%, as given in Table 4. These results indicate that the present model is capable to produce the behaviour of the combined cycle at different operating condition. It is expected that the obtained results from the gas turbine model to be greater than the actual ones because the present model has not considered all the losses.

RESULTS AND DISCUSSION

The performance of the power plant is investigated using the above equation (1 to 63). The MATLAB program is used to solve the equations and a function called X-Steam is used to get steam properties at different operating condition for all steam cycle. The following parameters are investigated:

1. **The effects of part loads operations:**

Figure 3 shows the operating part-loads performance obtained from the gas turbine model. The turbine operating parameters are controlled in such a way that turbine performance deterioration is minimized during the part-load operation. The VIGV position will be around 54% opening during the start up of the gas turbine and it will stay at its position during turbine loading up until turbine exhaust

temperature reaches the limit point (550℃ in the studied gas turbine). At that time the VIGV will be operating and opening more to maintain the turbine exhaust temperature within the allowable temperature limit.

Table 3 Main data for the thermodynamic simulation of the combined cycle at the design points

Unit	Parameter	Value
Compressor	i. Pressure loss of entry pressure	0.5%
	ii. Polytropic efficiency	90%
	iii. Mechanical efficiency	99%
	iv. Pressure ratio	13.9
Combustion chamber	i. Combustor efficiency	98%
	ii. Pressure loss of entry pressure	0.2%
	iii. Heat losses	2%
Gas turbine	i. Polytropic efficiency	95%
	ii. Exhaust pressure	1.113 bar
	iii. Turbine inlet temperature	1100˚C
HRSG	i. Effectiveness	94%
	ii. HP drum pressure	66 bar
	iii. HP feed water pressure	105 bar
	iv. LP drum pressure	4.6 bar
	v. LP feed water pressure	16.5 bar
	vi. HP pinch point temperature	10˚C
	vii. LP pinch point temperature	18˚C
Deaerator	Deaerator temperature	125˚C
Pumps	Isentropic efficiency	85%
LP pre-heater	i. Condensate water outlet temperature	85˚C
	ii. Condensate pressure	11.5 bar
Ejector	i. Steam entry pressure	15 bar
	ii. Steam mass flow rate	0.1 kg/s
Steam turbine	i. Minimum steam quality at exhaust	0.875
	ii. Isentropic efficiency	95%
	iii. Extraction steam pressure	0.85 bar
Air cooled condenser	i. Number of fans	16
	ii. Fan air volume flow rate	757 m^3/s
	iii. Total heat transfer surface area	619000 m^2
	iv. External diameter of tube	35 mm
	v. Tubes length	11.25 m
	vi. Fins outer diameter	73 mm
	vii. Fins thickness	0.3 mm
	viii. Fins pitch	2.8 mm
	ix. Distance between tubes in plane perpendicular to flow	54 mm
	x. Number of tubes	7840
	xi. Log mean temperature difference	15.35˚C

Once the turbine inlet temperature reaches the maximum allowable temperature (1100℃ in the studied gas turbine) the exhaust temperature will decay as the VIGV is varying to open more and admitting more air mass flow rate in the cycle.

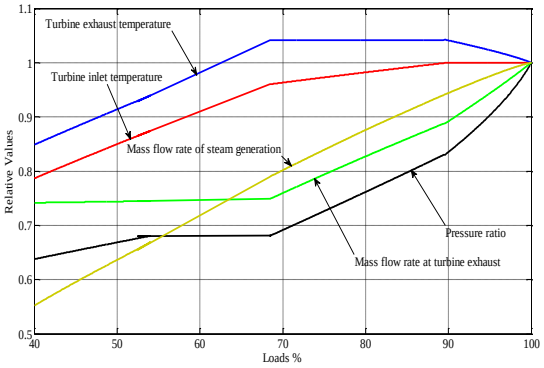

Figure 3 Part load performance of the gas turbine

In the present study a minimum gas turbine load of 40% is considered. This is the minimum load which a gas turbine can run in a case of combined cycle, as per the manufacture requirement.

Table 4 The comparison between the model results of the gas turbine with the corresponded ones given by the manufacture at the design point of gas turbine

%Load	Actual Load (MW)	Calculated Load (MW)	% Deviations
0	0	0	0
25	40	42.0347	5.087
50	81	84.0738	3.795
75	120	126.0861	5.072
80	131	136.1730	3.949
85	137	142.8976	4.305
90	145	151.3033	4.347
100	162	168.1148	3.775

The philosophy of a gas turbine is to control turbine inlet temperature and the exhaust temperature within the allowable limits of part load operation. Of course this will enhance the exhaust heat recovery for the bottom cycle as the gas turbine exhaust temperature is maintained at maximum value. This has been achieved by controlling the compressor inlet air mass flow rate by using VIGV variation when loads higher than 69%. [8].

The gas turbine operational characteristics can be classified into three zones as shown Figure 3. First zone occurs when the load is range of 0 to 69%. The turbine runs at conditions below the design value, and at this zone the VIGV will be opened at 53.85% and allows only 75% of the full load compressor inlet air mass flow rate.

Second zone occurs when the load is range of 69% to 90%, and at this zone the VIGV open will vary in order to control the exhaust gas temperature so it does go beyond the maximum allowable temperature which is 550˚C. To achieve that it admits more mass flow rate of air and fuel.

Third zone occurs when the load is above 90% to full load, and at this zone the turbine inlet temperature and other parameter are equal the design values.

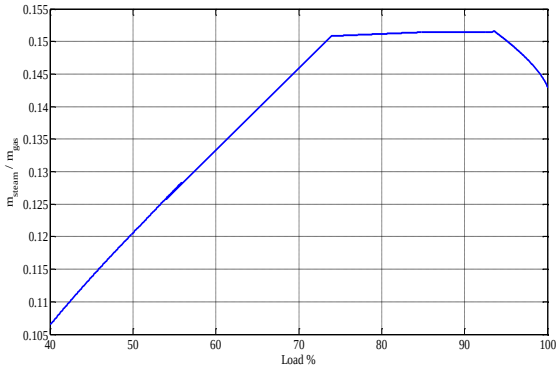

Figure 4 Ratio between steam generation and exhaust gas mass flow rate of gas turbine

Figure 4 shows the relation between the ratio of the steam mass flow rate and exhaust gases mass flow rate. As it is shown the steam ratio starts to increases linearly up to 74% load. This is due to: (a) the VIGV will be remained at 53.85% open, (b) the increase of fuel mass flow rate, and (c) a constant air mass flow rate. This is will lead to increase the turbine exhaust gases temperature. Therefore, the steam mass flow rate will increase as shown in Figure 4.

For loads range from 74% to 94% the exhaust gas turbine temperature reaches the maximum allowable temperature as shown in Figure 3. In this range, the ratio between steam mass flow rate and exhaust gases mass flow rate reaches the maximum value, as shown in Figure 4.

For loads above 94%, where the gas turbine controller tends to fix the inlet gas turbine temperature at the design value, the exhaust temperature will decay as a result of admitting more air mass flow rate to the combustion chamber by opening the VIGV more until becomes fully open. Therefore, the steam to gas mass ratio, in this zone, decreases, as shown in Figure 4.

Figure 5 shows the variation of relative exergy destruction rate in the compressor, combustion chamber and gas turbine with the load. The general trend, the relative ratio increases as the load increase. For the load of 69% of the full load the exergy destruction ratio relative to the full load one of: air compressor, combustion chamber and gas turbine is 60.9%, 79.6% and 59.3%, respectively. This behavior is due to the VIGV which is controlling the air mass flow rate entering the compressor. At the load of 90% the exergy destruction of air compressor, combustion chamber and gas turbine is 80.4%, 94.4% and 79.3% relative to the full load exergy destruction, respectively. The maximum destructions occurs in the combustion chamber.

The compressor and turbine exergy destruction are propotional to the air mass flow rate. Figure 3 indicates that the mas flow rate is decresed while load decreasing. While the combustion chamber exergy destruction is not affecting by the air mass flow rate it dependes the chemical reaction which is most significant source of exergy destruction than the thermo-mechanical exergy which are intering and leaving the combustion chamber.

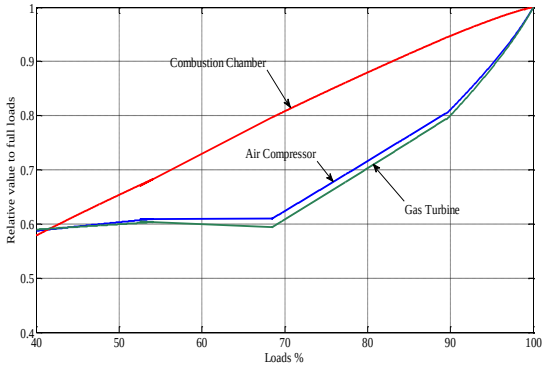

Figure 5 The effect of the loads on exergy destruction in compressor, combustion chamber and gas turbine

The same pattern was accomplished in the work of Baheta and Gilani [17]. It shows that variation of exergy destruction rate in the compressor and gas turbine are started to fall down from 20% load up to 50% load where the VSVs (Variable stator vanes) is fully opened. As the load reaches 50% the VSVs is started to closed which is caused to reduce the air mass flow rate entering the compressor.

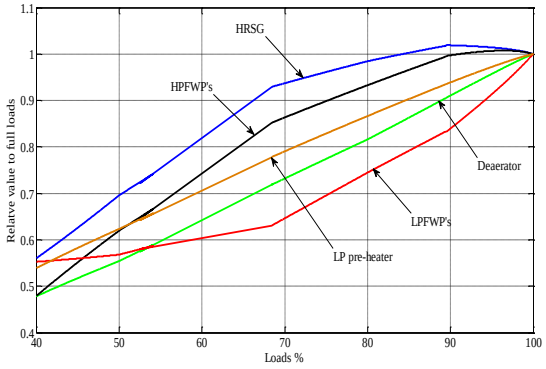

Figure 6 The effect of the loads on exergy destruction in HRSG

Figure 6 shows the effect of load on the exergy destruction rate, relative to the full load value, for the HRSG, deaerator, LP pre-heater, HPFWPs and LPFWPs. Form the figure it is clear that for all the exergy destruction is decreasing when the load decreases except for the HRSG is increasing at the range of 84.25% to 100% load. This last observation is due to the hot gases temperature which enters the HRSG is increased as the load increases as shown in Figure 3. Then, all components are decreasing as the load is decreased. Figure 7 shows the relative exergy destruction rate to full load for the steam turbine, ACC, CEP and ejector. The ejector exergy destruction rate is increasing as the load is decreased and it reaches its maximum value at load of 69%. The reason for that is the steam admitting to the ejector has a maximum temperature. This is causing the exergy destruction to increase as the load decreases. The steam

turbine exergy destruction rate is falling down to 60% relative to full at 70% load and then a minor reduction is occurred when the load is varying from 40% to 70%.

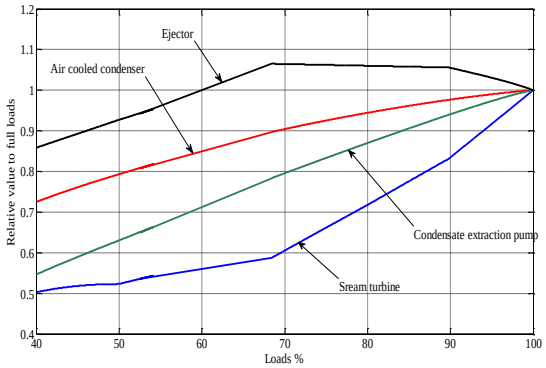

Figure 7 The effect of loads on exergy destruction in steam turbine

ACC and CEP exergy destruction rate is decreasing with load. The reason is the condensate mass flow rate plays the essential role of the exergy destruction and it is decreasing linearly with the load.

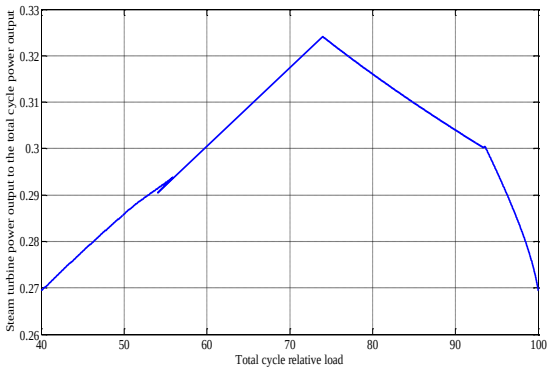

Figure 8 The effect of the load on the ratio of steam turbine power to the total block power

Figure 8 shows effect of the load on the ratio of steam turbine power to the total block power. The ratio is increasing as the load increases and it is reached to maximum at 74% of total cycle load. At this load the ratio of steam turbine power output is equal to 0.324 of the total block power output. By referring to Figure 3 it is cleared that at this point the turbine exhaust temperature is equal the maximum allowable temperature which is 550˚C and at the same time the exhaust gas mass flow rate is the minimum value. Consequently, the generated steam will reach its maximum temperature. In the other hand at loads greater than 74% the ratio of steam turbine power to the block one decreases as the load is increasing and this pattern agrees with the results of Figure 3.

The heat rate of the block is equal 7508 kJ/kWh at full load and it is dropped slightly by 0.49% when the total cycle load is 94%. Then, it has increased linearly by 2.5% when it reaches 74% load. When the load is less than 74% a sudden increased is observed as shown in Figure 9.

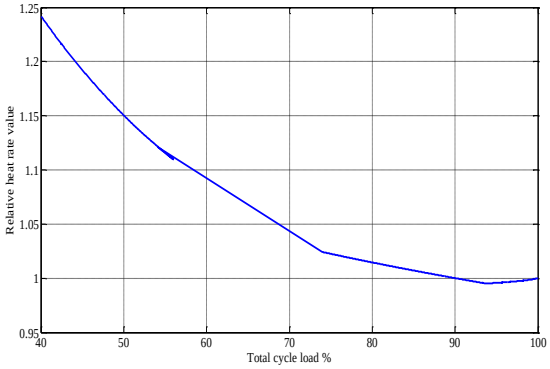

Figure 9 The effect of the loads on the heat rate (Relative values)

Figure 9 indicates that for the range of load 74% to 100% is the optimum range which the cycle operates without significant increase in the heat rate relative to the full load value. The minimum heat rate occurs at the full load of the block. It is important to run the block at the minimum heat rate because this will accompanied with less fuel consumption. This is lead to less emission and less green house gasses per kWh.

Table 5 Exergy destruction for all block elements at full load

Components	$\dot{E}_d$	η_{Exergy}	$y^*{}_d$	y_d
Compressor	17.73	91.37	6.28	3.45
Combustors	205.59	73.38	72.84	40.02
GT	10.51	97.26	3.73	2.04
HRSGs	18.06	84.38	6.40	3.52
Deaerator	1.47	91.15	0.26	0.14
HPFWP	0.18	88.95	0.03	0.02
LPFWP	0.02	87.19	0.01	0.002
ST	36.19	77.41	6.41	3.52
ACC	21.56	39.88	3.82	2.10
CEP	0.03	84.82	0.01	0.003
Ejector	0.08	95.45	0.01	0.01
LP Pre-Heater	1.18	80.91	0.21	0.11

Table 5 represents the exergy destruction, exergetic efficiency, exergy destruction rate, and exergy destruction ratio at full load. It shows that the higher exergy destruction rate is in combustion chamber which is 72.8% while the ACC exergy destruction rate is 3.8%. According to the first law of thermodynamics, energy losses associated with ACC is significant because it represent about 29.8% of the total energy input to the cycle and the results of the present work is agreed with the work of [16]. These results reflect the importance of more work to be carried out to investigate the reasons behind

the big destruction in the combustion chamber in order to reduce.

2. The effects of heat losses within the combustion chamber:

Figure 10 shows the effects of percentage of heat losses within the combustion chamber on the fuel consumption, gas turbine cycle efficiency and turbine work net compare to the case of nil heat losses. The heat losses is accounted by introducing the term (1-%HL) in the lift hand side of heat addition from the fuel Eq. 8. The fuel consumption increases linearly with increases of the percentage of heat losses. This is due to more fuel will be required to achieve the desired turbine inlet temperature (TIT). The extra fuel is added to compensate for the heat losses from the combustion chamber. In the present study, it has been assumed that the percentage of heat loss is varying from 0% to 5%. When the heat losses are 5% the fuel consumption increases by 5.87%, as shown in Figure 10.

As the fuel consumption is increasing, with the increasing of the percentage of heat losses, the gas turbine work net is increased too. Figure 10 shows that the relation between the percentage of heat loss and the gas turbine work net. The gas turbine work net increases slightly by 0.49% as the heat losses is increased by 5%. This small increase in gas turbine work net is very negligible. It is 0.8302 MW while the gas turbine full power is 162 MW. This is due to the increase of fuel mass flow rate enters to the gas turbine combustion chamber. This increase is to compensate the heat losses and consequently fix the inlet gas temperature to the turbine.

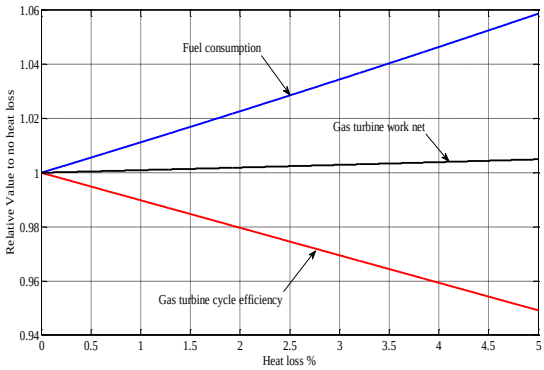

Figure 10 The effect of heat losses within combustion chamber on GT performance

In addition to that, Figure 10 shows that there is a drop in the cycle thermal efficiency with the increase in the heat losses. The cycle thermal efficiency drops by 5.08% when the heat loss is 5%. This observation reflects in the importance of reducing the heat losses in the combustion chamber by improving the insulation of the combustion chamber.

CONCLUSIONS

In the present study, the effects of varying the loads on the performance and exergy destruction of a combined cycle block consists of two gas turbine and one steam turbine have been demonstrated. To validate the present model, the gas turbine power at different loads is calculated. The model results are compared with the corresponding ones given by the block's manufacturer. The comparison shows the deviations to be in the range of 3-5%. The ratio of the steam turbine power to the block power reaches its maximum value of 0.324 at a load of 74%. This is corresponding to the maximum exhaust gasses temperature of 550 ° C. The results of the exergy destruction have shown that the highest destruction to be in the combustion chamber. This is because the chemical reactions are the most significant source of exergy destruction. The exergy destruction in the combustion chamber is mainly affected by the fuel mass flow. So, it can be reduced by preheating the inlet air and increasing the compressor pressure ratio i.e. increasing the temperature of the air entering the combustion chamber.

It has been observed that the heat rate of the plant is reached the lowest value when the block load is 94% of the full load. This is due to during part load the gas exhaust temperature increases slightly and reached the maximum allowable temperature i.e. improving the heat recovery steam generator.

The results of the heat losses in the combustion chamber have shown that it has a significant influence on the fuel mass flow rate. The fuel mass flow rate is increased as the heat losses within the combustion chamber increases. The maximum increase in the fuel consumption is 5.87% corresponding to a 5% heat losses. On the other hand, the work net of the gas turbine is slightly increased. Further, it causes a 5.07% reduction the thermal efficiency of the gas turbine.

REFERENCES

[1] M.Yilmazoglu,. and E. Amirbdedin, Second law and sensitivity analysis of a combined cycle power plant in Turkey, J. of Thermal Science and Technology, 2007, pp. 41-50.

[2] V. Wu. Nikulshin, and V. Nikulshing, Exergy efficiency calculation of energy intensive systems, Proceedings of ECOS,01, Istanbul, Turkey, 2001.

[3] P. Ahmadi and I. Dincer, Thermodynamic analysis and thermoeconomic optimization of dual pressure combined cycle power plant with a supplementary firing unit, *Energy conservation and Management*, Vol. 52, 2011, pp. 2296-2308.

[4] Sanjay, Investigation of effect of variation of cycle parameters on thermodynamic performance of gas-steam combined cycle, *Energy*; Vol. 36, 2011, pp. 157-167.

[5] B.V. Reddy and K. Mohamed, Exergy analysis of natural gas fired combined cycle power generation unit. I. J. of Exergy, 2007, pp 80-96.

[6] F. Haglind, Variable geometry gas turbine for improving the part-load performance of marine combined cycles – Gas turbine performance, *Energy*, Vol. 35, 2010, pp. 562-570.

[7] A. T. Baheta and S. I. Gilani, Exergy base performance analysis of gas turbine at part load conditions, *Journal of applied sciences*, Vol. 11, 2011, pp. 1994-1999.

[8] T. W. Song, J.L. Sohn, J.H. Kim and S.T. Ro, Exergy of the heavy-duty gas turbine in part-load operating conditions, *Exergy An International Journal*, Vol. 2, 2002, pp. 105-112.

[9] Stephen R. Turns, An Introduction to Combustion, Concepts and applications, Mc Graw-Hill, 2000.

[10] H.Cohen, GFC Rogers and HIH Saravabamuttoo, Gas Turbine Theory, Prentice Hall, 5th Ed., 2001.

[11] G.F Hewitt, G.L. Shires and T.R. Bott. Process Heat Transfer, Begell House Publishers, 1994.
[12] Y. A. Cengel and M. A. Boles. Thermodynamics, an engineering approach. 7th Ed., Mc Graw-Hill, 2011.
[13] M. J. Moran and H. N. Shapiro, Fundamentals of engineering thermodynamics. 6th Ed., J. Wiley, 2008.
[14] F. I. Adam, D. C. Onyejekwe and G. O. Unachukwu, The effect of ambient temperature on components performance of an in-service gas turbine plant using exergy method, *Singapore Journal of Scientific Research*, Vol. 1, 2011, pp. 23-37.
[15] Abusoglu A. and Kanoglu M., Exergoeconmic analysis and optimization of combined heat and power production, *Renewable and sustainable energy reviews*, Vol. 13, 2009, pp. 2295-2308.
[16] Aljundi I. H., Energy and exergy analysis of steam power plant in Jordan, *Applied thermal engineering*, Vol. 29, 2009, pp. 324-328.
[17] A. T. Baheta and S. I. U. Gilani, Exergy Based Performance Analysis of Gas Turbine at Part Load Conditions, *Journal of Applied Sciences*, Vol. 11, 2011, pp. 1994-1999.